JOURNAL

OF THE AMERICAN CHEMICAL SOCIETY

© Copyright 1987 by the American Chemical Society

VOLUME 109, NUMBER 12 JUNE 10, 1987

^{13}C NMR Studies of [1-^{13}C]Aldoses: Empirical Rules Correlating Pyranose Ring Configuration and Conformation with ^{13}C Chemical Shifts and ^{13}C–^{13}C Spin Couplings

Melinda J. King-Morris[†] and Anthony S. Serianni*[‡]

Contribution from Omicron Biochemicals Inc., Ithaca, New York 14850, and the Department of Chemistry, University of Notre Dame, Notre Dame, Indiana 46556. *Received July 3, 1986*

Abstract: Glycolaldehyde, DL-glyceraldehyde, D-erythrose, D-threose, D-arabinose, D-lyxose, D-ribose, D-xylose, D-allose, D-altrose, D-galactose, D-glucose, D-gulose, D-mannose, and D-talose have been synthesized and purified with [^{13}C]-enrichment (99 atom %) at the anomeric carbon. ^{13}C NMR spectra (75 MHz) of the natural and enriched compounds have been obtained in $^{2}H_2O$, from which ^{13}C–^{13}C couplings to the enriched sites were measured. On the basis of ^{13}C–^{13}C coupling patterns, ^{13}C chemical shifts for the aldoses were confirmed and some signals (e.g., talose) were reassigned. Complex spectra of enriched compounds were simplified by employing the INADEQUATE method of data collection (spectral editing), and signal assignments to specific tautomers were made in several cases with the aid of selective ^{13}C-decoupling. An empirical method has been developed that predicts ^{13}C chemical shifts in aldopyranose rings and has been used to examine the effect of pyranose structure on ^{13}C chemical shifts. The dependence of ^{13}C–^{13}C couplings involving C1 on furanose and pyranose ring configuration and conformation has been reexamined, and previous correlations have been modified to accommodate new data.

Aldofuranose and aldopyranose rings are important components of many biologically important compounds including oligo- and polysaccharides, oligo- and polynucleotides, coenzymes, and cell metabolites. The conformational properties of these rings in simple and complex structures have been largely determined by exploiting the well-known dependence of vicinal ^{1}H–^{1}H couplings ($^{3}J_{HH}$) on HCCH dihedral angles (Karplus relationships).[1] In some cases, however, $^{3}J_{HH}$ values are insufficient for an assignment of conformation, especially for furanoses,[2] and additional information obtained from one-, two-, and three-bond ^{13}C–^{13}C and ^{13}C–^{1}H couplings can be helpful. With modern multipulse NMR spectroscopy, these couplings can be obtained without the need for [^{13}C]-enrichment; for example, ^{13}C–^{13}C couplings can be measured from ^{13}C spectra obtained via double-quantum transitions (INADEQUATE),[3] but this method requires high sample concentrations and/or significant spectrometer time, and often it does not permit measurement of the more important longer range couplings. [^{13}C]-enriched molecules are still preferred when precise determinations of ^{13}C–^{13}C and ^{13}C–^{1}H couplings are required.[2,4,5]

In addition to studies of spin couplings, [^{13}C]-enriched carbohydrates have been used in conjunction with NMR and/or mass spectrometry to make unequivocal ^{1}H and ^{13}C NMR signal assignments,[2,4-8] establish solution composition (e.g., the presence of several equilibrating forms generated via tautomerization),[5,9-11] monitor the fate of an enriched carbon atom(s) during a reaction (chemical or enzymic) which may lead to the postulation of a reaction mechanism,[12-14] and elucidate metabolic pathways in living cells and organisms non-invasively.[15,16]

A pioneering study by Walker et al.[6] was reported in 1976 in which several [1-^{13}C]aldohexoses (D-glucose, D-mannose, D-galactose, L-fucose) were synthesized and examined by ^{13}C NMR (25 MHz). Useful correlations between pyranose ring structure/conformation and ^{13}C–^{13}C spin couplings were noted, albeit on a limited set of configurational isomers, and the utility of enriched compounds to make unequivocal ^{13}C signal assignments was emphasized. The aim of the present study is to extend this

[†] Omicron Biochemicals Inc.
[‡] University of Notre Dame.

(1) Karplus, M. *J. Chem. Phys.* **1959**, *30*, 11.
(2) Serianni, A. S.; Barker, R. *J. Org. Chem.* **1984**, *49*, 3292.
(3) Bax, A.; Freeman, R.; Kempsell, S. P. *J. Am. Chem. Soc.* **1980**, *102*, 4849.
(4) Hayes, M. L.; Serianni, A. S.; Barker, R. *Carbohydr. Res.* **1982**, *100*, 87.
(5) Snyder, J. R.; Serianni, A. S. *J. Org. Chem.* **1986**, *51*, 2694.
(6) Walker, T. E.; London, R. E.; Whaley, T. W.; Barker, R.; Matwiyoff, N. A. *J. Am. Chem. Soc.* **1976**, *98*, 5807.
(7) Barker, R.; Walker, T. E. *Meth. Carbohydr. Chem.* **1980**, *8*, 151.
(8) Snyder, J. R.; Serianni, A. S. *Carbohydr. Res.*, in press.
(9) Serianni, A. S.; Pierce, J.; Huang, S.-G.; Barker, R. *J. Am. Chem. Soc.* **1982**, *104*, 4037.
(10) Pierce, J.; Serianni, A. S.; Barker, R. *J. Am. Chem. Soc.* **1985**, *107*, 2448.
(11) Barker, R.; Serianni, A. S. *Acc. Chem. Res.* **1986**, *19*, 307.
(12) Hayes, M. L.; Pennings, N. J.; Serianni, A. S.; Barker, R. *J. Am. Chem. Soc.* **1982**, *104*, 6764.
(13) Serianni, A. S.; Nunez, H. A.; Barker, R. *J. Org. Chem.* **1980**, *45*, 3329.
(14) King-Morris, M. J.; Serianni, A. S. *Carbohydr. Res.* **1986**, *154*, 29.
(15) Neurohr, K. J.; Barrett, E. J.; Shulman, R. *Proc. Natl. Acad. Sci.* **1983**, *80*, 1603.
(16) Sacks, W.; Cowburn, D.; Bigler, R. E.; Sacks, S.; Fleischer, A. *Neurochem. Res.* **1985**, *10*, 201.

0002-7863/87/1509-3501$01.50/0 © 1987 American Chemical Society

Table I. Purification of Aldose C2-Epimers Generated by Cyanohydrin Reduction

parent aldehyde/aldose	product aldehyde/aldose[a]
formaldehyde	glycolaldehyde
glycolaldehyde	DL-glyceraldehyde
D-glyceraldehyde	D-threose, D-erythrose
D-erythrose	D-arabinose, D-ribose, PA
D-threose	D-xylose, D-lyxose
D-arabinose	D-glucose, D-mannose, PA
D-lyxose	D-galactose, PA, D-talose
D-ribose	D-altrose, D-allose
D-xylose	PA, D-idose, D-gulose

[a] Product aldoses are listed in order of elution from Dowex 50 × 8 (200–400 mesh) (Ca^{2+}).[25] In some cases, the elution position of unreacted parent aldehyde/aldose (PA) is given. Column fractions were assayed for reducing sugar with phenol–sulfuric acid.[26]

previous study to D-[1-^{13}C]aldotetroses, aldopentoses, and the remaining aldohexoses, which were prepared by using a cyanohydrin reduction method[17,18] developed subsequent to the Walker report. The short-chain hydroxyaldehydes, [1-^{13}C]glycolaldehyde and DL-[1-^{13}C]glyceraldehyde, have also been prepared. With these enriched aldoses, we have sought to verify ^{13}C chemical shift assignments,[19] evaluate some modern NMR methods to interpret ^{13}C spectra of enriched sugars, and develop an empirical method to predict ^{13}C chemical shifts with reasonable accuracy in aldopyranose rings. In addition, enriched compounds have been used to detect minor tautomers (linear aldehyde and hydrate) in aqueous solution and to reassess the structural factors that affect the magnitudes of ^{13}C–^{13}C spin couplings between C1 and the remaining pyranosyl and furanosyl ring carbons.

Experimental Section

Materials. Formaldehyde (37% w/w aqueous solution) was purchased from Fisher Chemical Co. and used without further assay or purification. Glycolaldehyde, D-arabinose, D-lyxose, D-ribose, D-xylose, D-galactose, D-glucose, D-mannose, D-fructose, and Dowex ion-exchange resins were purchased from Sigma Chemical Co. D-Glyceraldehyde,[20] D-erythrose,[21] and D-threose[22] were prepared from D-fructose, 4,6-*O*-ethylidene-D-glucose, and 4,6-*O*-ethylidene-D-galactose, respectively. Potassium [^{13}C]cyanide (K[^{13}C]N, 99 atom % ^{13}C) and deuterium oxide ($^{2}H_2O$, 98 atom % ^{2}H) were obtained from Cambridge Isotope Laboratories.

Instrumentation. Broad-band ^{1}H-decoupled ^{13}C NMR spectra (75 MHz) were obtained at ambient temperature (~28 °C) on a Nicolet NT-300 300-MHz FT–NMR spectrometer operating with quadrature-phase detection and equipped with a 293B pulse programmer. Spectra of enriched compounds were obtained by block-averaging FIDs, which were processed with a double-exponential filter (chosen empirically to maximize resolution by line-narrowing) and zero-filled to 32K real points (to maximize digital resolution) prior to fourier transformation. A spectral width of 5000 Hz (~65 ppm) was used with the transmitter offset at 84 ppm (i.e., 51–117 ppm spectral range). Relaxation delays (2–3 s) and 60–70° observation pulses were used to minimize spin-saturation due to incomplete relaxation between pulses. Spectra were referenced externally to the C1 chemical shift of β-D-[1-^{13}C]glucopyranose (97.4 ppm), and chemical shifts are accurate to ±0.1 ppm. ^{13}C–^{13}C coupling constants are accurate to ±0.1 Hz.

Selective ^{13}C-decoupled ^{13}C NMR spectra (^{13}C{^{13}C} spectra) were obtained with the aid of a heteronuclear decoupling accessory (F3 decoupler unit) purchased from GE NMR Systems. 1D INADEQUATE ^{13}C NMR spectra[3] were obtained with pulse-programming software supplied by GE NMR Systems.

Synthesis of [1-^{13}C]Aldoses. [1-^{13}C]Aldoses were synthesized from parent aldoses and K^{13}CN by the cyanohydrin reduction method described in previous reports.[17,18] The protocol involves the condensation of K^{13}CN with an aldose[23] at pH 7.2–7.5 to give C2-epimeric [1-^{13}C]-cyanohydrins in ~90% yield. The cyanohydrins were reduced in situ with 5% Pd/$BaSO_4$ and H_2 to give the corresponding C2-epimeric [1-^{13}C]aldoses in 75–80% yield. The specific conditions of these reactions (i.e., reagent stoichiometry and concentrations, pH, H_2 pressure) vary with cyanohydrin structure.[24] The parent aldoses and the products generated by them are identified in Table I.

Separation of the C2-epimeric pairs of [1-^{13}C]aldoses (~10 mmol total sugar) was accomplished by chromatography on a 2.5 × 80 cm column of Dowex 50 × 8 (200–400 mesh) in the calcium form[25] (Table I). A 15 × 100 cm column was used to separate D-gulose and D-idose. Fractions were assayed for reducing sugar with phenol–sulfuric acid,[26] and those containing sugar were pooled and the solutions concentrated

Chart I

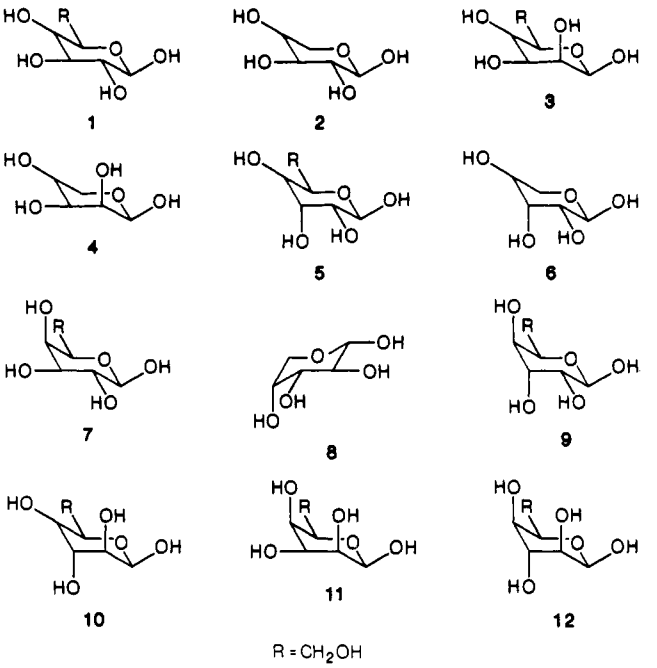

Chart II

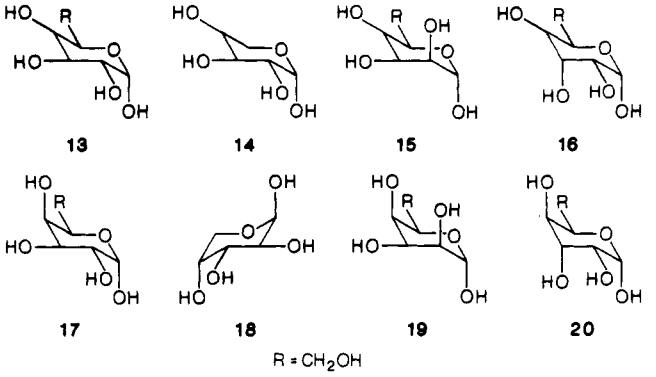

Chart III

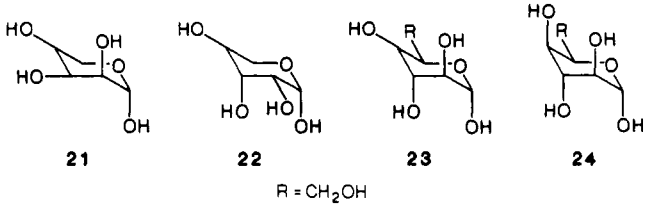

(17) Serianni, A. S.; Nunez, H. A.; Barker, R. *Carbohydr. Res.* **1979**, *72*, 71.

(18) Serianni, A. S.; Barker, R. "Synthetic Approaches to Carbohydrates Enriched with Stable Isotopes of Carbon, Hydrogen and Oxygen", In *Isotopes in the Physical and Biomedical Sciences*; Jones, J., Buncel, E., Eds.; Elsevier: New York, 1987, in press.

(19) Bock, K.; Pedersen, C. *Adv. Carbohydr. Chem. Biochem.* **1983**, *41*, 27.

(20) Perlin, A. S. *Meth. Carbohydr. Chem.* **1962**, *1*, 61.

(21) Perlin, A. S. *Meth. Carbohydr. Chem.* **1962**, *1*, 64.

(22) Ball, D. H. *J. Org. Chem.* **1966**, *31*, 220.

(23) In the preparation of [1-^{13}C]hexoses, a 3:1 ratio of CN:parent aldose is required to effect >90% conversion to nitrile. A 1:1 stoichiometry is used for the synthesis of labeled glycolaldehyde, glyceraldehyde, tetroses, and pentoses. See ref 24.

(24) Serianni, A. S.; Nunez, H. A.; Hayes, M. L.; Barker, R. *Meth. Enzymol.* **1982**, *89*, 64.

(25) Angyal, S. J.; Bethell, G. S.; Beveridge, R. *Carbohydr. Res.* **1979**, *73*, 9.

(26) Hodge, J. E.; Hofreiter, B. T. *Meth. Carbohydr. Chem.* **1962**, *1*, 380.

at 30° in vacuo to ~20 mL. After deionization by separate and batchwise treatment with Dowex 1 (OAc^-) and Dowex 50 (H^+), aldose concentrations were determined by hypoiodite oxidation.[27] Aldose solutions were then passed through small columns (0.5 × 2 cm) of Dowex chelating resin (20–50 mesh) (H^+) and appropriate aliquots were taken to prepare 0.5–0.7 M solutions in ^2H_2O for ^{13}C NMR analysis.

Synthesis of Unenriched Aldoses. Several unenriched hexoses (D-altrose, D-allose, D-gulose, D-talose) required for this study were not available commercially or were prohibitively expensive. The above protocol for the preparation of [1-^{13}C]aldoses was used with unenriched KCN to prepare these compounds.

Results and Discussion

A. Configurational/Conformational Correlations in the Aldoses. An analysis of aldopyranose ^{13}C NMR parameters (i.e., chemical shifts, ^{13}C–^{13}C couplings) is facilitated by identifying the structural correlations that exist in these compounds. The latter are derived from a knowledge of preferred conformations determined from previous ^1H NMR studies and by calculations of conformational energies.[28,29] Pyranoses **1–20** in Charts I and II are shown in their preferred chair conformations and are considered conformationally "fixed"; those in Chart III (**21–24**) exist in both $^4C_1$ and $^1C_4$ conformations and are thus conformationally "flexible".

In the β-aldopyranoses (Chart I), gluco **1** and xylo **2** have the same ring configuration and conformation ($^4C_1$). As a consequence, it may be expected that ^{13}C chemical shifts and ^{13}C–^{13}C couplings may be similar in **1** and **2**. Likewise, β-manno **3** and β-lyxo **4**, β-allo **5** and β-ribo **6**, and β-galacto **7** and α-arabino **8** have the same relative configuration, although **7** assumes a $^4C_1$ conformation and **8** prefers $^1C_4$.[29] Aldopentose–aldohexose structural correlations do not exist for β-gulo **9**, β-altro **10**, β-talo **11**, and β-ido **12**.

In the α-aldopyranoses (Chart II), gluco **13** and xylo **14** and gal **17** and β-arabino **18** have the same relative configuration, although, like **7** and **8** in Chart I, **17** and **18** assume alternate chair conformations. α-Talo **19** and α-gulo **20** do not have configurational relatives in the aldopentopyranoses. α-Manno **15** and α-allo **16** are related configurationally to α-lyxo **21** and α-ribo **22**, but the latter pentopyranoses along with α-altro **23** and α-ido **24** (Chart III) are conformationally flexible due to the presence of two or more axial OH groups in both chair forms,[5,29] and comparisons are not valid. NMR parameters observed for **21–24**, therefore, must be interpreted in light of this conformational heterogeneity.

The aldohexose D-idose is not discussed in this study, as the ^1H and ^{13}C NMR spectra of this aldose have been thoroughly investigated in a previous report.[5]

B. Basic Features of ^{13}C Spectra of [1-^{13}C]-Enriched Aldoses. The ^{13}C NMR spectrum of a [1-^{13}C]-enriched aldose differs from the spectrum of the natural compound in two important ways: the signals of the C1 carbons (enriched region) are more easily detected and thus more intense than the remaining carbon signals, and the unenriched region contains signal multiplicities due to ^{13}C–^{13}C coupling to the enriched C1 carbons (e.g., in 99 atom % enriched compounds, C2 will nearly always be adjacent to a ^{13}C nucleus at C1 and therefore its signal will appear as a doublet). These ^{13}C–^{13}C couplings can be obtained from natural abundance spectra (INADEQUATE),[3] but here one-bond couplings are detected mainly to provide a carbon connectivity map for structural elucidation; in general the smaller two- and three-bond couplings[30] of importance to conformational studies are not obtained with precision. The application of INADEQUATE methods *with enriched compounds*, however, can simplify complex spectra and aid in their interpretation (see below).

Enrichment of aldoses at the anomeric carbon allows easier detection, identification, and quantitation of aldose tautomers in solution, especially those present in low abundance (e.g., hydrate and aldehyde).[5,9,10] For example, the ^{13}C spectrum of D-[1-^{13}C]ribose (Figure 1) in ^2H_2O shows the presence of four major tautomers, two furanoses and two pyranoses. While facilitated by [^{13}C]-enrichment, the proportions of these major forms can be determined adequately from the ^{13}C spectrum of the unenriched compound. However, the linear aldehyde can also be detected (C1 resonance at 204.5 ppm) and quantified (~0.05 mol %) in the enriched spectrum, a result not obtainable with natural material.

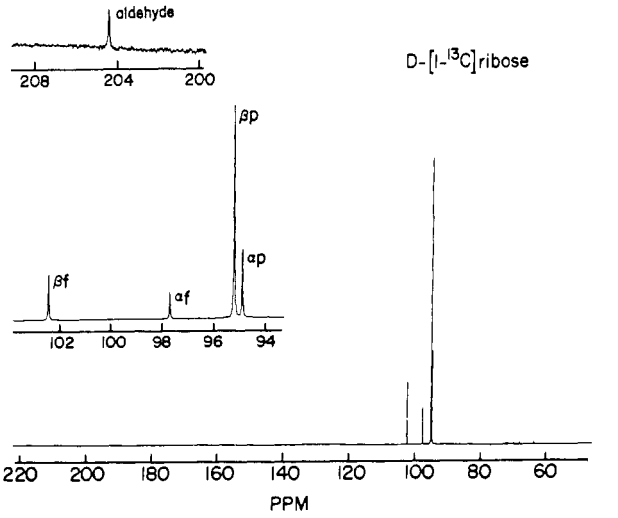

Figure 1. The ^1H-decoupled ^{13}C NMR spectrum (75 MHz) of D-[1-^{13}C]ribose in ^2H_2O, showing only the enriched carbons. The intense signals are assigned to α- and β-ribofuranoses and α- and β-ribopyranoses as shown. The weak signal at 204.5 ppm is attributed to the C1 signal of the aldehyde form, present at ~0.05 mol·% at 25 °C.

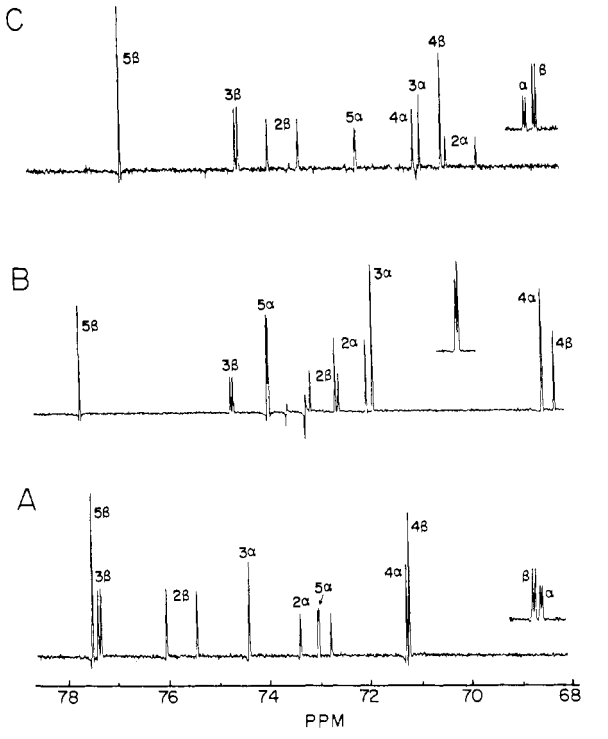

Figure 2. The ^1H-decoupled ^{13}C NMR spectra (75 MHz) of D-[1-^{13}C]glucose (A), D-[1-^{13}C]mannose (B), and D-[1-^{13}C]galactose (C) in ^2H_2O. The unenriched region of each spectrum is shown with carbon assignments for each pyranose form. Inset signals are from the C6 carbons, which resonate at ~63 ppm. The out-of-phase signals are an artefact caused by quadrature phase detection.

^{13}C spectra (unenriched regions) of D-[1-^{13}C]glucose, D-[1-^{13}C]mannose, and D-[1-^{13}C]galactose in ^2H_2O are shown in Figure 2. The assignment of the C2 signal of each pyranose anomer is made unequivocally by observation of $^1J_{C1,C2}$ (~45 Hz) and

(27) Schaffer, R.; Isbell, H. S. *Meth. Carbohydr. Chem.* **1963**, *2*, 11.
(28) Eliel, E. L.; Allinger, N. L.; Angyal, S. J.; Morrison, G. A. *Conformational Analysis*; Interscience: New York, 1967; pp 351–432.
(29) Angyal, S. J. *Angew. Chem., Int. Ed. Engl.* **1969**, *8*, 157.
(30) Marshall, J. L. *Carbon–Carbon and Carbon-Proton NMR Couplings: Applications to Organic Stereochemistry and Conformational Analysis*; Verlag Chemie, Weinheim/Bergstr., Germany, 1983.

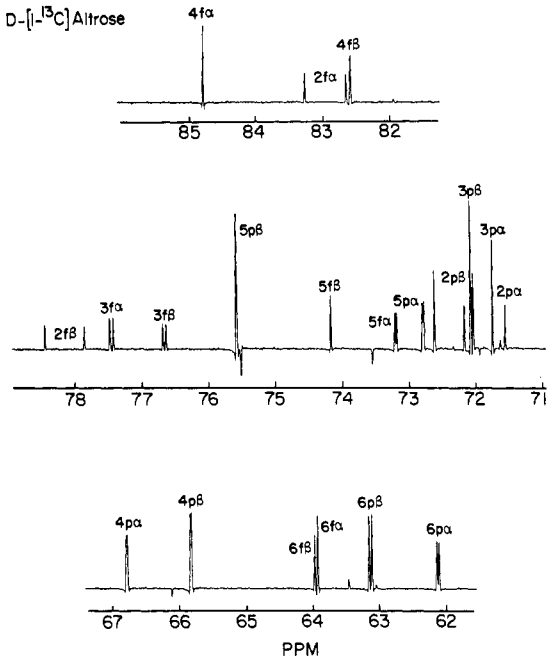

Figure 3. The ^{1}H-decoupled ^{13}C NMR spectrum (75 MHz) of D-[1-^{13}C]altrose in ^2H_2O, showing only the unenriched region. Carbon assignments for α- and β-furanoses and α- and β-pyranoses are as shown. Note the small splitting of C4 of both pyranoses caused by coupling to C1.

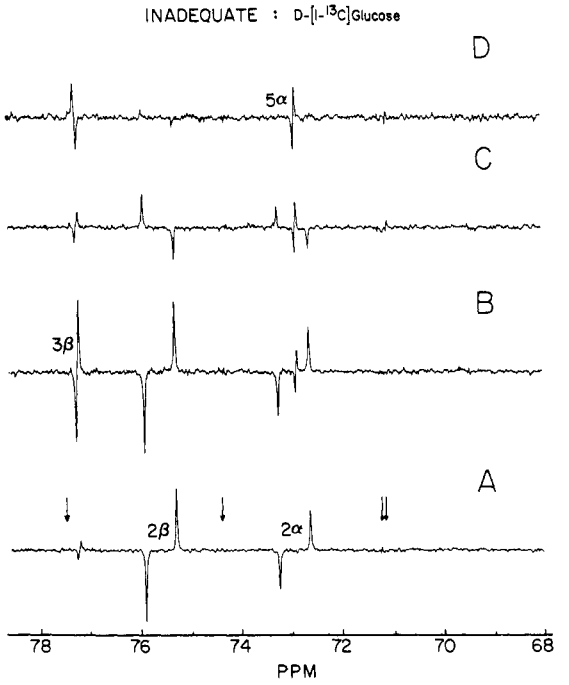

Figure 4. INADEQUATE spectra obtained on D-[1-^{13}C]glucose in ^2H_2O, showing the effect of mixing time on signal detection. Only the C2–C5 region of the spectrum is shown. Mixing times are 5.4 ms (A), 50 ms (B), 100 ms (C), and 130 ms (D). In spectrum A only C2 carbons are detected, since the experiment is optimized to detect via one-bond ^{13}C–^{13}C couplings. As the mixing time is increased, carbons with smaller longer range couplings (i.e., C3 and C5) appear, while C2 carbons are suppressed. Carbons which are not coupled to C1 are completely suppressed with this technique.

from relative intensities; in the case of similar intensities, selective ^{13}C decoupling of C1 can be used to correlate C1 with C2 for each form, as illustrated recently for apiose.[31] As discussed below, C1–C3 and C1–C5 coupling in pyranoses depends on ring configuration, whereas C1–C4 coupling is almost always absent (except in the altropyranoses, Figure 3). As a consequence, the assignments of C3, C4, and C5 based solely on observed coupling to C1 are only as firm as the empirical rules that relate structure to coupling magnitudes; at a minimum, previous assignments may be consistent or inconsistent with these observed couplings. Coupling between C1 and C6 is observed in all aldohexopyranoses but is not needed for assignment purposes, except when distinguishing C6 resonances of tautomers present in nearly equal abundance (accomplished via homonuclear ^{13}C decoupling[31]). However, $^3J_{C1,C6}$ is a useful probe of pyranosyl ring conformation.[4,6]

The pyranosyl rings of glucose, mannose, and galactose are considerably more stable than furanosyl rings and linear forms having these configurations, and thus comprise >90% of the total forms present in aqueous solution at 25 °C.[29] This is also true for xylose, lyxose, arabinose, gulose, and allose. However, solutions of ribose, talose, idose, and altrose contain substantial amounts of furanose forms,[5,29] and their ^{13}C spectra are more complex. For example, the spectrum of D-[1-^{13}C]altrose (Figure 3) contains 20 signals (unenriched region) from two furanose and two pyranose forms. Some of these signals are split by coupling to C1; for example, in α-D-[1-^{13}C]altropyranose **23**, C2, C4, C5, and C6 are coupled in C1.

^{13}C NMR spectra of [1-^{13}C]-enriched aldoses can be simplified by detecting double-quantum transitions only, that is, by acquiring INADEQUATE spectra.[3] Spectra acquired in this manner contain signals due *only to those carbons coupled to C1* (Figure 4). Depending on the choice of mixing times, the detection of signals can be limited to those carbons adjacent to the enriched site or to those separated by two or more bonds from this site. Spectral editing of this sort is useful in simplifying spectra of complex monomeric (see Figure 5B), oligomeric, or polymeric substances containing one or more [^{13}C]-enriched sites.

C. The Assignment and Prediction of ^{13}C Chemical Shifts. A compilation of ^{13}C chemical shifts of aldofuranoses and aldo-

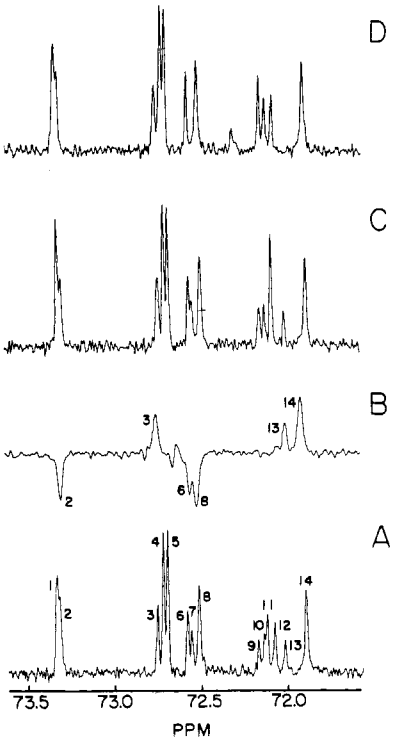

Figure 5. (A) The ^{1}H-decoupled ^{13}C NMR spectrum (75 MHz) of D-[1-^{13}C]talose in ^2H_2O showing only the 71.5–73.5-ppm region that contains signals from several carbons of furanose and pyranose tautomers. (B) An INADEQUATE spectrum of the same region, optimized to detect only C2 carbons. Signals 2–3, 6–13, and 8–14 are due to C2 of β-pyranose, β-furanose, and α-pyranose, respectively. (C) The same region after decoupling C1 of the α-furanose. Signals 11 and 12, which have collapsed to a singlet, are due to C3 of this tautomer. (D) The same region after decoupling C1 of the β-furanose. Signals 9–10 (C3) and 6–7 (C5) have collapsed, and signals 6–13 (C2) are partly decoupled.

(31) Snyder, J. R.; Serianni, A. S. *Carbohydr. Res.*, in press.

Table II. ^{13}C Chemical Shifts[a] of the Aldoses

compound	chemical shift (ppm)					
	C1	C2	C3	C4	C5	C6
glycolaldehyde hydrate	91.2	66.0				
glyceraldehyde hydrate	91.3	75.6	63.5			
D-erythrose						
α-furanose	97.0	72.6	70.8	73.0		
β-furanose	102.6	77.8	71.9	72.6		
hydrate	91.0	75.1	73.2	64.0		
D-threose						
α-furanose	103.6	82.2	76.6	74.4		
β-furanose	98.1	77.7	76.3	71.9		
hydrate	91.4	74.8	72.4	64.5		
D-arabinose						
α-pyranose	98.2 (97.9)	73.4 (73.4)	74.0 (74.3)	70.0 (70.2)	67.9	
β-pyranose	94.1 (93.6)	70.0 (70.4)	70.1* (71.3)	70.2* (70.8)	64.0	
D-lyxose						
α-pyranose	95.5	71.46	72.0	69.0	64.6	
β-pyranose	95.9 (95.2)	71.52 (72.7)	74.2 (74.5)	68.0 (68.1)	65.7	
D-ribose						
α-furanose	97.8	72.4	71.50	84.5	62.9	
β-furanose	102.4	76.7	71.9	84.0	64.0	
α-pyranose	95.0	71.52	70.7	68.8	64.5	
β-pyranose	95.3 (94.9)	72.5 (72.8)	70.4 (72.7)	68.7 (68.3)	64.5	
D-xylose						
α-pyranose	93.7 (93.6)	73.0 (72.6)	74.3 (74.2)	70.9 (71.1)	62.4	
β-pyranose	98.1 (97.4)	75.5 (75.6)	77.3 (77.2)	70.7 (71.1)	66.7	
D-allose						
α-pyranose	94.3 (94.3)	68.6 (69.8)	73.2 (73.2)	67.6 (68.3)	68.3 (70.6)	62.3
β-pyranose	94.9 (94.9)	72.8 (72.8)	72.7 (72.7)	68.3 (68.3)	75.1 (75.1)	62.8
D-altrose						
α-furanose	102.7	83.0	77.4	84.8	73.2	63.9
β-furanose	96.9	78.1	76.7	82.6	74.2	64.0
α-pyranose	95.3	71.9	71.8	66.8	72.8	62.1
β-pyranose	93.3 (92.7)	72.3 (72.3)	72.1 (72.1)	65.8 (65.3)	75.6 (75.3)	63.1
D-galactose						
α-pyranose	93.6 (93.6)	69.8 (70.4)	70.7 (71.3)	70.8 (70.8)	72.0 (72.1)	62.7
β-pyranose	97.9 (97.9)	73.4 (73.4)	74.3 (74.3)	70.2 (70.2)	76.6 (76.6)	62.5
D-glucose						
α-pyranose	93.6 (93.6)	73.0 (72.6)	74.2 (74.2)	71.14 (71.1)	72.9 (72.9)	62.1
β-pyranose	97.4	75.6	77.2	71.09	77.4	62.3
D-gulose						
α-pyranose	94.4 (94.3)	66.3 (67.6)	72.4 (73.3)	71.0 (71.6)	68.0 (69.8)	62.5
β-pyranose	95.4 (95.4)	70.7 (70.6)	72.8 (72.8)	71.0 (71.0)	75.3 (74.3)	62.6
D-mannose						
α-pyranose	95.5 (95.5)	72.2 (72.2)	71.7 (71.5)	68.4 (68.1)	73.9 (73.1)	62.5
β-pyranose	95.2 (95.2)	72.7 (72.7)	74.5 (74.5)	68.1 (68.1)	77.6 (77.6)	62.5
D-talose						
α-furanose	102.4	76.7	72.09	83.3	73.3	64.3
β-furanose	98.0	72.3	72.15	83.9	72.6	64.4
α-pyranose	96.1 (95.5)	72.2 (72.5)	66.6 (68.6)	71.1 (70.8)	72.6 (72.3)	63.0
β-pyranose	95.6 (95.7)	73.0 (73.0)	69.9 (71.6)	70.1 (70.2)	77.1 (76.8)	62.7

[a] Values are referenced (external) to the anomeric carbon signal of β-D-glucopyranose (97.4 ppm) and are accurate to ±0.1 ppm. Values in parentheses are calculated chemical shifts obtained with the use of Table III. Assignments marked with an asterisk are uncertain.

pyranoses has been published recently by Bock and Pedersen.[19] We have reexamined these assignments in view of the ^{13}C–^{13}C coupling patterns observed in enriched spectra; in all cases but one, the assignments (Table II) are consistent with coupling trends. The exception is D-talose, whose spectrum had been assigned previously by Pfeffer[32] and Angyal.[33] Splittings observed in the ^{13}C spectrum of D-[1-^{13}C]talose suggest that the C2 and C3 assignments of the β-pyranose **11** are reversed; Angyal[33] found a similar error for the α-pyranose **19**. Other talose assignments were suspect, especially signals found in the most complex region of the spectrum (71–74 ppm, Figure 5A). To sort this region out, the INADEQUATE method was applied to select for C2 carbons (Figure 5B). Further information was provided by separately saturating the enriched C1 signals of the α- and β-talofuranoses; several unenriched signals could then be correlated with each furanose form by observing their collapse to singlets. Using these data, we have reassigned the talose spectrum (Table II).

Firm chemical shift assignments are essential for most NMR studies of carbohydrates. As a corollary, it is important to understand how ^{13}C chemical shieldings are affected by carbohydrate structure. An empirical method that predicts these values may provide some insight into this problem.

In this study, ^{13}C spectra of the complete set of D-aldopyranoses have been obtained under *similar experimental conditions*, permitting a confident comparison of chemical shifts necessary to identify potential empirical relationships. It is worth noting that in configurationally related pentopyranose–hexopyranose pairs (e.g., **1** and **2**), there is good agreement between corresponding ^{13}C chemical shifts (Table II), suggesting that a systematic treatment of chemical shift data in Table II may lead to a useful set of predictive rules. We have devised a formula (Table III) to calculate ^{13}C chemical shifts for aldopyranose rings. This formula is based on a set of "core chemical shifts" for each ring carbon, with separate values for each OH orientation (axial or equatorial) at that carbon whose shift is to be calculated, with OH groups equatorial at the remaining ring carbons. These "core" values are modified if axial OH groups are present. For example, to calculate the C2 chemical shift of β-D-gulopyranose **9**, a "core

(32) Pfeffer, P. E.; Valentine, K. M.; Parrish, F. W. *J. Am. Chem. Soc.* **1979**, *101*, 1265.
(33) Angyal, S. J.; Trans, T. Q. *Aust. J. Chem.* **1983**, *36*, 937.

Table III. Empirical Rule for the Calculation of Carbon Chemical Shifts in the Aldopyranoses[a]

ring carbon		carbon with axial OH[c]			
		C1	C2	C3	C4
C1	(a) α-glc (93.6)[b]		1.9	0.7	0.0
	(e) β-glc (97.4)		−2.2	−2.5	0.5
C2	(a) β-man (72.7)	−0.5		−0.4	0.3
	(e) β-glc (75.6)	−3.0		−2.8	−2.2
C3	(a) β-all (72.7)	0.5	−0.6		0.1
	(e) β-glc (77.2)	−3.0	−2.7		−2.9
C4	(a) β-gal (70.2)	0.6	0.0	0.8	
	(e) β-glc (71.1)	0.0	−3.0	−2.8	
C5	(e) β-glc (77.4)	−4.5	0.2	−2.3	−0.8

[a] $^4C_1$ conformers. [b] "Core chemical shifts" (in ppm) are given in parentheses for each ring carbon attached to an axial (a) or equatorial (e) hydroxyl group. [c] "Core chemical shift" modifiers (in ppm) where (+) signs are added to "core chemical shifts"; (−) values are subtracted.

chemical shift" of 75.6 ppm (Table III) (the actual chemical shift of C2 of β-D-glucopyranose **1** (Table I) where all OH groups are equatorial) is modified to account for axial OH groups at C3 and C4, that is, values of 2.8 and 2.2 ppm are *subtracted* from this "core" value to obtain a predicted value of 70.6 ppm.[34] The actual value is 70.7 ppm. With the use of this formula, chemical shifts have been calculated for several aldopyranoses and are given in Table II (values in parentheses). On the average, actual and calculated values differ by about 0.3 ppm. Larger deviations occur mainly in structures that are conformationally flexible (these rules apply to $^4C_1$ conformers only) or possibly where non-ideal chair conformers are present.

By formulating "core chemical shift" modifiers as in Table III, an observation emerges that bears upon the relationship between pyranose structure and ^{13}C chemical shifts. It appears that pyranosyl ring carbons that bear axial OH groups are relatively insensitive (±0.5-ppm shifts) to configuration at other ring carbons. In contrast, carbons bearing equatorial OH groups are sensitive (−3 ppm shifts) to structure at α and β carbons and consistently become more shielded as the number of adjacent axial OH groups increases. In other words, the electron density around a pyranosyl ring carbon bearing an equatorial OH group appears to be more affected by changes in nearby hydroxyl group orientation than the same carbon bearing an axial OH group. The reason for this behavior is obscure, but theoretical studies (e.g., ab initio MO calculations) may provide some insight. In practical terms, it is logical to suggest that the considerable carbon chemical shift dispersion (~10 ppm) observed for aldopyranose ring carbons (C2–C5) is due primarily to the sensitivity of those carbons bearing equatorial OH substituents to overall structure; in the absence of this differential behavior, one might expect pyranosyl ring carbons to resonate over a more limited spectral range, making ^{13}C spectra less useful for structural elucidation.

D. ^{13}C–^{13}C Coupling Constants. ^{13}C–^{13}C coupling constants observed in [1-^{13}C]aldoses are given in Table IV. In configurationally related pentopyranose–hexopyranose pairs (e.g., **1** and **2**), there is good agreement between corresponding ^{13}C–^{13}C couplings. To facilitate an analysis of these values, aldopyranoses and aldofuranoses will be discussed separately.

Aldopyranoses. According to Walker et al.,[6] $^1J_{C1,C2}$ for aldopyranose anomers in which O2 is equatorial will be similar; for example, $^1J_{C1,C2}$ in α-D-glucopyranose **13** (46.2 Hz) is similar to that in β-D-glucopyranose **1** (46.0 Hz), and the same is true galactopyranose anomers. Mannopyranose and talopyranose anomers in which O2 is axial exhibit greater differences between anomers (~4.1 Hz), consistent with previous rationalizations.[6,7] A problem, however, arises for allo and gulo configurations where significant differences (~1.9 Hz) are observed between anomers (Table IV) despite an equatorial orientation of O2. This apparent discrepancy cannot be attributed to conformational heterogeneity, as these aldopyranoses highly prefer the $^4C_1$ chair form.[29] It would appear that configuration at O3 (axial in allo and gulo isomers) also affects the magnitude of $^1J_{C1,C2}$.

An alternate way to view this problem emphasizes the differences in sensitivity of $^1J_{C1,C2}$ to configuration at C2 and C3 between pyranose anomers. $^1J_{C1,C2}$ in α-pyranoses is less sensitive than that in β-pyranoses to structure at C2 and C3; values of 46.6, 46.1, and 45.7 Hz are observed in α-manno **15**, α-gluco **13**, and α-allo **16**, respectively, for an overall *decrease* of 0.9 Hz. In the same series, $^1J_{C1,C2}$ values of 42.5, 46.0, and 47.5 Hz are observed for β-anomers, for an overall *increase* of 5.0 Hz. The greater and

Table IV. ^{13}C Coupling Constants[a] in the Aldoses

compound	coupled nuclei				
	C1,C2	C1,C3	C1,C4	C1,C5	C1,C6
glycolaldehyde hydrate	48.4				
glyceraldehyde hydrate	48.5	2.5			
D-erythrose					
α-furanose	43.2	1.2	nc		
β-furanose	46.8	3.0	nc		
hydrate	48.2	~1.2	2.2		
D-threose					
α-furanose	46.1	2.9	nc		
β-furanose	42.5	2.7	nc		
hydrate		nc	2.5		
D-arabinose					
α-pyranose	45.7	4.2	nc	nc	
β-pyranose	45.7	nc	nc	2.1	
D-lyxose					
α-pyranose	47.1	nc	nc	1.3	
β-pyranose	43.2	2.7	nc	nc	
D-ribose					
α-furanose	42.6	2.2	nc	2.0	
β-furanose	46.1	3.3	nc		
α-pyranose	43.2	1.1	nc	obs	
β-pyranose	47.0	br	nc	obs	
D-xylose					
α-pyranose	46.1	nc	nc	2.0	
β-pyranose	45.9	4.0	nc	nc	
D-allose					
α-pyranose	45.4	2.4	nc	obs	2.9
β-pyranose	47.3	nc	nc	nc	3.3
D-altrose					
α-furanose	46.3	4.0	nc	2.0	nc
β-furanose	43.8	3.4	nc	nc	nc
α-pyranose	46.2	nc	1.0	1.6	2.4
β-pyranose	43.9	nc	1.3	nc	3.2
D-galactose					
α-pyranose	46.0	nc	nc	1.9	3.6
β-pyranose	45.9	4.6	nc	nc	4.4
D-glucose					
α-pyranose	46.2	nc	nc	1.8	3.3
β-pyranose	46.0	4.5	nc	nc	4.1
D-gulose					
α-pyranose	45.9	2.0	obs	1.9	3.2
β-pyranose	47.7	nc	nc	nc	3.7
D-mannose					
α-pyranose	46.7	nc	nc	2.0	obs
β-pyranose	42.7	4.0	nc	nc	obs
D-talose					
α-furanose	46.1	obs	nc	3.2	nc
β-furanose	42.3	1.7	nc	2.5	nc
α-pyranose	46.5	nc	nc	1.8	3.3
β-pyranose	42.3	3.9	nc	nc	4.2

[a] Values are reported in Hz and are accurate to ±0.1 Hz. The entries "nc" and "obs" denote *n*o *c*oupling and *obs*cured *s*ignals, respectively. The entry "br" denoted *br*oadened resonance.

(34) The "core chemical shift" for a given carbon site in a pyranose ring is, by definition, equal to the observed chemical shift when all hydroxy groups at the remaining ring carbons are *equatorial*. For example, the "core chemical shift" for C3 when O3 is equatorial is equal to the chemical shift observed for C3 in β-D-glucopyranose; alternately, the "core chemical shift" for C3 when O3 is axial is equal to the chemical shift observed for C3 in β-D-allose. To calculate chemical shifts, these "core" values are modified to account for the presence of axial OH groups in the pyranose ring under consideration, as illustrated in the text. The modifiers given in Table III were obtained by determining the difference in observed chemical shifts between appropriate configurations. For example, the C1 chemical shift modifier of −2.2 (for an axial O2) was obtained by comparing the C1 chemical shift of β-glc to that of β-man; likewise, the modifier of −2.5 (for an axial O3) was obtained by comparing the C1 chemical shift of β-glc to that of β-D-allo.

opposing (relative to α-pyranoses) response of $^1J_{C1,C2}$ in β-pyranoses to changes in ring structure, therefore, generates the observed differences in coupling between anomers. As noted above, the *chemical shifts* of carbons bearing equatorial OH groups also appear to be more sensitive to structure; electron density changes at these carbons would affect both chemical shieldings and internuclear couplings, making these observations internally consistent. In practical terms, $^1J_{C1,C2}$ is not presently a reliable probe of anomeric configuration in aldopyranoses, in marked contrast to the behavior of $^1J_{C1,C2}$ in furanoses (see below).

According to Walker et al.,[6] only α-pyranoses ($^4C_1$ conformers) should exhibit coupling between C1 and C5. In structural terms, $^2J_{C1,C5}$ occurs when both C2 and O1 are gauche to C5 (α-anomers) and is absent when C2 is gauche and O1 trans (β-anomers). This correlation is substantiated from data in Table IV, that is, $^2J_{C1,C5}$ in β-pyranoses is essentially zero while couplings of 1.3–2.0 Hz are observed in α-pyranoses.

The magnitude of $^2J_{C1,C3}$ in aldopyranoses depends not only on the orientation of O1 relative to C3 but also on the orientation of O3 relative to C1.[6] The largest coupling is expected when O1, C1, C2, C3, and O3 are coplanar. In aldopyranoses in which O3 is equatorial, β-anomers have greater couplings (3.9–4.6 Hz) than α-anomers (0 Hz) (Table IV), since O1 and O3 are antiperiplanar to C3 and C1, respectively, in the former. In aldopyranoses in which O3 is axial, it may be expected (as proposed previously[6]) that coupling in β-anomers will decrease. This predicted decreased coupling is observed, as $^2J_{C1,C2}$ in allo **5**, ribo **6**, gulo **9**, and altro **10** is essentially zero (Table IV).

The "abnormal" $^2J_{C1,C3}$ values observed in several aldopyranoses are probably due to the effects of conformational averaging. The smaller value for β-lyxo **4** (observed 2.7 Hz) would result if the $^1C_4$ conformer (where $^2J_{C1,C3}$ should be zero) contributed to the observed value. Likewise, in α-ribo **22**, α-allo **16**, and α-gulo **20**, the observed values of 1.1–2.4 Hz probably reflect a contribution from the $^1C_4$ conformer in which maximal coupling should occur.

Coupling between C1 and C4 in aldopyranose rings is determined by two through-bond pathways, namely, C1–O5–C5–C4 and C1–C2–C3–C4; this dual-pathway coupling is denoted as $^{3+3}J_{C1,C4}$. The failure to observe this coupling in pyranoses[6] is considered to result from these two component couplings having similar magnitudes but opposite signs.[30] In the altropyranoses, $^{3+3}J_{C1,C4}$ is observed in both α- (1.0 Hz) and β-pyranoses (1.3 Hz). By considering the more conformationally stable β-pyranose ($^4C_1$), it is clear that the only difference between altro **10** and gluco **1** isomers (in which no C1–C4 coupling is observed) is the substituent geometry along the C1–C2–C3–C4 coupling pathway. The diaxial orientation of O2 and O3 in β-altro must change (either increase or decrease by ~1.0 Hz) the coupling along this path such that the algebraic sum is no longer zero.

$^3J_{C1,C6}$ is observed in all D-aldopyranoses ($^4C_1$ conformers), with values for β-anomers somewhat larger than those for α-anomers. Since C1 and C6 are antiperiplanar in both anomers, this dependence suggests that the orientation of O1 with respect to the coupling pathway is important, that is, greater coupling occurs when O1, C1, O5, C5, and C6 are coplanar. The 2.4-Hz coupling for α-D-[1-^{13}C]altropyranose **23** probably reflects a contribution from the $^1C_4$ conformer in which C1 and C6 are gauche and coupling is expected to be smaller (~1.5 Hz).

Aldofuranoses. The conformational flexibility inherent to furanose rings[2] makes the structural interpretation of NMR parameters in these systems difficult. Nevertheless, several notable ^{13}C–^{13}C coupling trends can be discerned.

$^1J_{C1,C2}$ values in aldofuranoses are sensitive to anomeric configuration. Compounds having O1–O2 cis give consistently smaller couplings (42.9 ± 0.6 Hz) than those having O1–O2 trans (46.3 ± 0.3 Hz). This correlation has been noted previously in other furanose anomers[2,8] and can be considered a reliable parameter for structure elucidation in these rings.

Coupling between C1 and C3 varies from 1.7 to 4.0 Hz and is determined by two through-bond pathways, C1–C2–C3 and C1–O4–C4–C3. On the other hand, C1–C4 coupling, which is determined by C1–C2–C3–C4 and C1–O4–C4 coupling pathways, is nearly zero in all furanose rings studied to date.[2,8,31] Further analysis of these dual-pathway couplings awaits the determination of coupling signs and the conformational properties of these molecules.

$^3J_{C1,C5}$ (2.0–3.2 Hz) is observed in some pento- and hexofuranoses (Table IV). These values suggest dihedral angles in the range 130–140° between C1 and C5, consistent with a quasiequatorial orientation of C5.

Summary

A comprehensive examination of the ^{13}C NMR spectral characteristics of [1-^{13}C]aldoses has been presented in this paper. In most cases, one-dimensional spectra (75 MHz) in ^2H_2O were amenable to interpretation. In some instances, notably when several tautomers are present in comparable amounts in solution, INADEQUATE spectroscopy and selective ^{13}C-decoupling facilitated the analysis. The INADEQUATE method of data acquisition is particularly useful for editing complex spectra, that is, to selectively detect ^{13}C nuclei based on their magnitudes of coupling to C1. This approach should be valuable in studies of selectively [^{13}C]-enriched oligomers and polymers in general, where spectral complexity can be significantly reduced without the loss of useful information (i.e., ^{13}C–^{13}C couplings to the enriched site(s)).

Further support has been provided for previous empirical rules relating J_{CC} to pyranose ring configuration and conformation. In several cases ($^1J_{C1,C2}$ and $^3J_{C1,C6}$ in pyranoses), the additional data have resulted in the modification of these rules. The heretofore unobserved coupling between C1 and C4 ($^{3+3}J_{C1,C4}$) has now been found in pyranoses (altropyranoses), implying that configurational factors play an important role in determining its magnitude. In all, these data should provide a firmer basis on which to interpret ^{13}C–^{13}C couplings in other carbohydrate systems, especially oligosaccharides and polysaccharides.

The observed structural trends in ^{13}C–^{13}C couplings in pyranose rings have provided a means to verify/reassign ^{13}C chemical shifts. Reasonable predictions of these values were obtained by using an empirical method devised in this study. This method provides a means to *verify* assignments and should by no means be used to make assignments in the absence of more definitive tests. The formulation of this method has been used mainly to provide some insight into the structural features that determine ^{13}C shifts in pyranoses.

Minor tautomers of the aldoses (e.g., ribose) in solution were detected by ^{13}C NMR with [1-^{13}C]-enrichment, even when these constituents comprise 0.05 mol % of the mixture (e.g., ribose aldehyde). Studies in progress with D-[1-^{13}C]glucose and D-[1-^{13}C]xylose, whose solutions are expected to contain even less aldehyde form, will address the problem of limits to the detection and quantification of these minor forms with use of enriched compounds.[35]

Acknowledgment. This work was supported by the Research Corporation (10028), the National Institutes of Health (GM 33791), and Omicron Biochemicals Inc. of Ithaca, New York. The authors thank Rosemary Patti for typing the manuscript.

Registry No. Formaldehyde, 50-00-0; glycoaldehyde, 141-46-8; D-glyceraldehyde, 453-17-8; D-erythrose, 583-50-6; D-threose, 95-43-2; D-arabinose, 10323-20-3; D-lyxose, 1114-34-7; D-ribose, 50-69-1; D-xylose, 58-86-6; [1-^{13}C]glycoaldehyde, 71122-42-4; [1-^{13}C]-DL-glyceraldehyde, 70849-18-2; [1-^{13}C]-D-threose, 70849-20-6; [1-^{13}C]-D-erythrose, 70849-19-3; [1-^{13}C]-D-arabinose, 70849-23-9; [1-^{13}C]-D-ribose, 70849-24-0; [1-^{13}C]-D-xylose, 70849-21-7; [1-^{13}C]-D-lyxose, 70849-22-8; [1-^{13}C]-D-glucose, 40762-22-9; [1-^{13}C]-D-mannose, 70849-31-9; [1-^{13}C]-D-galactose, 70849-30-8; [1-^{13}C]-D-talose, 70849-29-5; [1-^{13}C]-D-altrose, 70849-27-3; [1-^{13}C]-D-allose, 70849-28-4; [1-^{13}C]-D-idose, 70849-26-2; [1-^{13}C]-D-glucose, 70849-25-1; glycolaldehyde hydrate, 40460-44-4; glyceraldehyde hydrate, 107890-68-6; α-D-erythrofuranose, 72599-80-5; β-D-erythrofuranose, 72599-81-6; D-erythrose hydrate, 107890-69-7;

(35) Dynamic range affects the ability to detect small signals in the presence of large signals by NMR. This range can be extended by both software and hardware modifications (e.g., block-averaging, use of double-precision data processing, 16-bit data collection).[11]

α-D-threofuranose, 80877-72-1; β-D-threofuranose, 80877-73-2; D-threose hydrate, 107890-70-0; α,γ-D-arabinopyranose, 608-45-7; β-D-arabinopyranose, 6748-95-4; α-D-lyxopyranose, 608-46-8; β-D-lyxopyranose, 608-47-9; α-D-ribofuranose, 32445-75-3; β-D-ribofuranose, 36468-53-8; α-D-ribopyranose, 7296-59-5; β-D-ribopyranose, 7296-60-8; α-D-xylopyranose, 6763-34-4; β-D-xylopyranose, 2460-44-8; α-D-allopyranose, 7282-79-3; β-D-allopyranose, 7283-09-2; α-D-altrofuranose, 41846-93-9; β-D-altrofuranose, 40461-79-8; α-D-altropyranose, 7282-80-6; β-D-altropyranose, 7283-10-5; α-D-galactopyranose, 3646-73-9; β-D-galactopyranose, 7296-64-2; α-D-glucopyranose, 492-62-6; β-D-glucopyranose, 492-61-5; α-D-glucopyranose, 7282-78-2; β-D-glucopyranose, 7283-08-1; α-D-mannopyranose, 7296-15-3; β-D-mannopyranose, 7322-31-8; α-D-talofuranose, 51076-04-1; β-D-talofuranose, 41847-63-6; α-D-talopyranose, 7282-81-7; β-D-talopyranose, 7283-11-6.

Cesium-133 Solid-State Nuclear Magnetic Resonance Spectroscopy of Alkalides and Electrides

Steven B. Dawes, Ahmed S. Ellaboudy, and James L. Dye*

Contribution from the Department of Chemistry, Michigan State University, East Lansing, Michigan 48824. *Received August 15, 1986*

Abstract: ^{133}Cs MAS-NMR spectra were measured for alkalides and electrides that contain complexed cesium cations and, in one case, the cesium anion. The chemical shifts of the cesium cations in alkalides of $Cs^+(15C5)_2$ and $Cs^+(18C6)_2$ are +27 ± 3 and −60 ± 2 ppm, respectively, except for $Cs^+(18C6)_2{\cdot}Cs^-$, which shows temperature-dependent chemical shifts through two phase changes. The shifts range from −40 to −50 ppm for $Cs^+(18C6)_2$ and from −205 to −240 ppm for Cs^-. Depending on the method of preparation, the NMR spectrum of compounds prepared from cesium and cryptand[2.2.2], C222, show either one or two peaks, which correspond to the inclusive and exclusive complexed cations. Since all samples are essentially diamagnetic, the anions could be Cs^- ions broadened beyond detection limits, trapped electrons that are spin-paired, or mixtures of ceside and electride. The paramagnetic electride $Cs^+(18C6)_2{\cdot}e^-$ shows a temperature-dependent Knight shift due to unpaired electron density at the cesium nucleus. The fractional atomic character of Cs^+ is only 3.3×10^{-4}, in agreement with the view that electrons are trapped at anionic sites well away from Cs^+. A compound of mixed anionic stoichiometry, $Cs^+(18C6)_2{\cdot}Na^-_xe^-_{1-x}$, was prepared from solutions with the nominal values $x = 0.2$ and 0.8 and gives four temperature-dependent paramagnetic peaks in addition to a peak caused by precipitation of the pure iodide. The four peaks indicate that sodium anions can substitute for electrons in up to three of the eight nearest anionic sites about a complexed cation. This shows that each electron in $Cs^+(18C6)_2{\cdot}e^-$ interacts with all eight of its cationic neighbors and is not preferentially localized on one of them.

Complexed cations, formed from simple alkali metal cations and crown ethers or cryptands, are sufficiently stable to reduction that salts with alkali metal anions ($M^+C{\cdot}N^-$, known as alkalides) or with electrons at the anionic sites ($M^+C{\cdot}e^-$, known as electrides) can be formed. The first alkalide, $Na^+C222{\cdot}Na^-$ (C222 = cryptand[2.2.2]), was synthesized in 1974[1] and has been characterized by single-crystal X-ray diffraction,[2] optical spectroscopy,[3,4] powder conductivity,[5] and more recently by photoelectron emission and fluorescence spectroscopy.[6] The nature of the sodium anion was best characterized by NMR, first in solutions of $Na^+C222{\cdot}Na^-$ in ethylamine,[7,8] THF and methylamine,[8] and later in the solid state with polycrystalline $Na^+C222{\cdot}Na^-$.[9] Other NMR studies of Na^- in solution[10-13] showed that the chemical shift of this anion in each case was the same as the chemical shift calculated for Na^- in the gaseous state.[14-16] Thus, the sodium anion was shown to be a genuine spherical anion with a filled 3s orbital that is not strongly affected by its environment.[17] Similar conclusions resulted from NMR studies of K^-, Cs^-, and Rb^- in solution.[8,13,18,19]

To date more than 40 alkalide and electride compounds have been synthesized, and magic angle sample spinning NMR (MAS-NMR) has become a primary technique for their characterization. The oxidation state of an ion or element in a compound is easily identified by the chemical shift of the resonance. The cationic and anionic species in an alkalide, which always contains two alkali metal nuclei, can often be properly identified by NMR. Signals have been detected in the solid state for $Na^+{\cdot}C$ and Na^-,[9,20] K^-,[18] Rb^-,[21] and $Cs^+{\cdot}C$ and Cs^-.[22,23] In these expressions, C represents a cryptand such as C222 or a crown ether, such as 18-crown-6 (18C6) or 15-crown-5 (15C5).[24] No signal was detected for either K^+C^{18} or $Rb^+{\cdot}C^{21}$ because of extreme quadrupolar line broadening that could not be reduced by MAS.

In addition to the identification of alkali metal cations and anions in alkalides and electrides by measurement of the chemical

(1) Dye, J. L.; Ceraso, J. M.; Lok, M. T.; Barnett, B. L.; Tehan, F. J. *J. Am. Chem. Soc.* **1974**, *96*, 608.
(2) Tehan, F. J.; Barnett, B. L.; Dye, J. L. *J. Am. Chem. Soc.* **1974**, *96*, 7203.
(3) Dye, J. L.; Yemen, M. R.; DaGue, M. G.; Lehn, J.-M. *J. Chem. Phys.* **1978**, *68*, 1665.
(4) Le, L. D.; Issa, D.; Van Eck, B.; Dye, J. L. *J. Phys. Chem.* **1982**, *86*, 7.
(5) Dye, J. L.; *Angew. Chem. Int. Ed. Engl.* **1979**, *18*, 587.
(6) Jaenicke, S.; Dye, J. L. *J. Solid State Chem.* **1984**, *54*, 320.
(7) Ceraso, J. M.; Dye, J. L. *J. Chem. Phys.* **1974**, *61*, 1985.
(8) Dye, J. L.; Andrews, C. W.; Ceraso, J. M. *J. Phys. Chem.* **1975**, *79*, 3076.
(9) Ellaboudy, A.; Tinkham, M. L.; Van Eck, B.; Dye, J. L.; Smith, P. B. *J. Phys. Chem.* **1984**, *88*, 3852.
(10) Edwards, P. P.; Guy, S. C.; Holton, D. M.; McFarlane, W. *J. Chem. Soc., Chem. Commun.* **1981**, 1185.
(11) Edwards, P. P.; Guy, S. C.; Holton, D.; Johnson, D. C.; Sienko, M.; McFarlane, W.; Wood, B. *J. Phys. Chem.* **1983**, *87*, 4362.
(12) Edwards, P. P. *J. Phys. Chem.* **1984**, *88*, 3772.
(13) Holton, D. M.; Edwards, P. P.; Johnson, D. C.; Page, C. S.; McFarlane, W.; Wood, B. *J. Am. Chem. Soc.* **1985**, *107*, 6499.
(14) Dickinson, W. C. *Phys. Rev.* **1950**, *80*, 563.
(15) Malli, G.; Fraga, S. *Theor. Chim. Acta* **1966**, *5*, 275.
(16) Pyper, N. C., Edwards, P. P. *J. Am. Chem. Soc.* **1986**, *108*, 78.
(17) Dye, J. L. *Prog. Inorg. Chem.* **1984**, *32*, 327.
(18) Tinkham, M. L.; Dye, J. L. *J. Am. Chem. Soc.* **1985**, *107*, 6129.
(19) Edwards, P. P.; Ellaboudy, A. S.; Holton, D. M. *Nature (London)* **1985**, *317*, 242.
(20) Ellaboudy, A.; Dye, J. L. *J. Magn. Reson.* **1986**, *66*, 491.
(21) Tinkham, M. L.; Ellaboudy, A.; Dye, J. L.; Smith, P. B. *J. Phys. Chem.* **1986**, *90*, 14.
(22) Ellaboudy, A.; Dye, J. L.; Smith, P. B. *J. Am. Chem. Soc.* **1983**, *105*, 6490.
(23) Dye, J. L.; Ellaboudy, A. *Chem. Brit.* **1984**, *20*, 210.
(24) IUPAC names: 18-crown-6, 1,4,7,10,13,16-hexaoxacyclooctadecane, abbreviation 18C6; 15-crown-5, 1,4,7,10,13-pentaoxacyclopentadecane, abbreviation 15C5; cryptand[2.2.2], 4,7,13,16,21,24-hexaoxa-1,10-diazabicyclo[8.8.8]hexacosane, abbreviation C222.

0002-7863/87/1509-3508$01.50/0 © 1987 American Chemical Society